DOI 10.1007/s10812-016-0352-8
*Journal of Applied Spectroscopy, Vol. 83, No. 4, September, 2016 (Russian Original Vol. 83, No. 4, July–August, 2016)*

# SIMULTANEOUS DETERMINATION OF AMILORIDE AND HYDROCHLOROTHIAZIDE IN A COMPOUND TABLET BY DIFFUSE REFLECTANCE SPECTROSCOPY AND CHEMOMETRICS

**J. Tang, X. Li, Y. Feng, and B. Liang***

UDC 543.42:615.45

*This paper studies the simultaneous determination of amiloride hydrochloride (AMH) and hydrochlorothiazide (HCTZ) in amiloride hydrochloride tablets by ultraviolet-visible-shortwave near-infrared diffuse reflectance spectroscopy (UV-Vis-swNIR DRS) and chemometrics. Quantitative models for the two components were established by partial least squares (PLS) and support vector regression (SVR), respectively. For the PLS models of AMH and HCTZ, the determination coefficient $R^2$ of the calibration set was 0.9503 and 0.9538, and the coefficient $R^2$ of the prediction set was 0.8983 and 0.9260, respectively. The root mean square error of the calibration set (RMSEC) was 0.8 mg and 8.1 mg, while the root mean square error of the prediction set (RMSEP) was 1.0 mg and 8.7 mg, respectively. For the SVR models of AMH and HCTZ, the $R^2$ of the calibration set was 0.9668 and 0.9609; the $R^2$ of the prediction set was 0.9145 and 0.9446, respectively. The RMSEC was 0.7 and 7.5 mg, and the RMSEP was 0.9 and 8.9 mg, respectively. The results show that SVR modeling has a satisfactory prediction effect. The proposed method based on UV-vis-swNIR and chemometrics is efficient, nondestructive, and expected to be used for online quality monitoring in the production of drugs.*

***Keywords:*** *compound amiloride hydrochloride tablet, partial least squares, support vector regression, ultraviolet-visible-shortwave near-infrared diffuse reflectance spectroscopy.*

**Introduction.** Process analytical technology (PAT), as a developing trend of new, good manufacturing practice (GMP), has been proposed and promoted by the FDA in order to control the quality of drug manufacturing. The analytical methods suitable for PAT in the pharmaceutical industry should meet the following criteria: be accurate and precise; require minimal sample pretreatment in order to ensure a high throughput; allow simultaneous determination of several analytes; provide control of the manufacturing process; adhere to GMP standards [1]. Therefore, it is vital to develop simple and efficient analytical techniques for PAT.

A compound amiloride hydrochloride tablet, the active components of which are amiloride hydrochloride (AMH) and hydrochlorothiazide (HCTZ), is widely used as a diuretic and antihypertensive drug. A number of analytical methods have been developed for the simultaneous determination of these components in mixtures, among which are liquid chromatography (LC) [2–4], liquid chromatography/tandem mass spectrometry [5, 6], high-performance thin-layer chromatography (HPTLC) [7], spectrophotometric methods [8–10], UV/chemometry [11, 12], capillary electrophoresis [13], and the differential pulse polarographic methods [14]. High-performance liquid chromatography (HPLC) is mostly used to quantitatively determine the two components with reliable results. However, these methods are all carried out in solutions, which needs complex and time-consuming sample pretreatment.

UV-vis-swNIR DRS is a spectral analytical technique based on measuring the output light that provides information on the structure and composition of samples through multiple interactions of the incident light with internal molecules. Samples do not need pretreatment, which makes it a widely used analytical technique in many areas, including the analysis of catalytic materials [15], the analysis of the chemical properties of soil [16], the identification of cancer [17, 18], the prediction of the harvest period of apples [19], and the study of the transdermal kinetics of drugs [20]. However, UV-Vis-swNIR DRS is seldom used in the determination of solid drugs and has not received the attention it deserves. We have recently reported on two studies, the ultraviolet-visible diffuse reflectance spectroscopy (UV-Vis DRS) support vector regression (SVR) method

*To whom correspondence should be addressed.

College of Chemical Engineering, Sichuan University, Chengdu, 610065, China; e-mail: liangbing@sina.com.

Abstract of article is published in Zhurnal Prikladnoi Spektroskopii, Vol. 83, No. 4, p. 669, July–August, 2016.

 

for determination of the content of cimetidine tablets [21], and the qualitative and simultaneous quantitative analysis of cimetidine polymorphs by UV-Vis-swNIR DRS and multivariate calibration models [22]. These studies demonstrate the potential of UV-vis-swNIR DRS and UV-Vis DRS in the determination of solid drugs.

The diffuse reflectance spectra of complex samples such as pharmaceutical preparations often have a significant overlap. Therefore, it is hard to analyze the spectra data by conventional calculation. Chemometrics can solve this problem by multivariate calibration, optimizing the process of chemical measurement and extracting useful information from the measurement data. Multivariate calibration is a useful tool in the analysis of multicomponent mixtures because it allows simultaneous determination of each component in the mixture, with minimum sample preparation and reasonable accuracy [10].

With the development of computer science, chemometric methods such as PLS, principal component regression (PCR), and SVR are increasingly used in the quantitative analysis of complex mixtures. PLS regression is a method for building regression models between the independent variable ($X$) and the dependent variable ($Y$), which is based on bilinear decomposition of the calibration matrix. This technique constructs new predictor variables (components) as the linear combinations of the original predictor variables. PLS constructs these components while considering the observed response values, leading to a parsimonious model. The most important feature of PLS is that the successively computed score vectors have the property of maximum covariance with the unexplained part of the dependent variable [23]. However, PLS is a linear regression method, which makes it difficult to achieve regression and prediction when dealing with a complex nonlinear problem, while SVR, a relatively new kind of regression method proposed in the 1990's, can solve this problem to some extent. SVR is based on the principle of minimizing the structural risk. The core idea of this modeling is to map low-dimensional data into a high-dimensional feature space for linear regression through a nonlinear mapping. With the introduction of the ε insensitive function, SVR has been successfully used for nonlinear regression and function approximation [24].

There are still no reports on the application of UV-vis-swNIR DRS in the simultaneous determination of active components. Therefore, the aim of our study is to investigate the feasibility of applying UV-Vis-swNIR DRS and chemometrics in the simultaneous quantification of active pharmaceutical components. In the study, two algorithms of PLS and SVR were applied, and their performance was compared.

**Material and Methods.** AMH with a purity of 99.31% and HCTZ with a purity over 99% were bought from Yan Shan Chemical Ltd., Hangzhou and HongXinKang Fine Chemical Ltd., Wuhan, respectively. Soluble starch, sodium carboxymethyl starch and magnesium stearate, purchased from Kelong Chemical Reagent Factory, Chengdu and dextrin obtained from Bo Di Chemical Ltd., Tianjin were of analytical grade.

The bulk drug powder was weighed by a JY2002 electronic analytical balance (Shanghai Precision Scientific instrument Co., Ltd.). Tabletting was performed by a ZPS008 rotary tablet press (Shanghai Tianxiangjiantai Pharmaceutical Machinery Co., Ltd.). UV-Vis diffuse reflectance spectra were acquired using an S2000 Optical Fiber Spectrometer (Hangzhou Sizhi Technology Co., Ltd.) controlled by Spectra Pro-Analysis Version 3.2 software, equipped with a light source (Ocean Optics, USA), a linear silicon CCD array detector (TCD Toshiba 1304), and a Y-type optical fiber probe. Spectral data were processed by MATLAB R2014a software, version 8.3 (The Math Works, Natick, USA) and Unscrambler software, version 9.7 (CAMO Software, AS).

AMH, HCTZ, and the excipients including soluble starch, sodium carboxymethyl starch, magnesium stearate, and dextrin were dried for 1 h at 105°C, then ground and sieved, mixed evenly, divided into 28 powder samples of different content levels, and compressed into 222 artificial tablets with a diameter of 9.0 mm, a thickness of 4.2 mm, and a weight of 300 mg per tablet by the direct compression method. The percentages of AMH and HCTZ per tablet varied from 1.1% to 5.7% and 10.5% to 54.7%, respectively. A calibration set of 150 tablets and a prediction set of 72 tablets were obtained by random selection.

Each artificial tablet was placed in a sample cell, with the optical fiber probe placed vertically on the upper surface of the tablet. Each tablet was measured three times under the following conditions: scan range from 200 to 1106 nm, exposure time 293 ms, and resolution 3.3 nm, with Spectralon as background reference. The average of the three measured spectra was treated as the spectral data of the tablet.

**Results and Discussion.** UV-vis-swNIR diffuse reflectance spectra of the active component and excipient are shown in Fig. 1. Here, the absorbance is defined as the negative logarithm of the relative diffuse reflectance rate of samples, calculated as follows:

$$A = \log (1/R\infty) , \quad (1)$$

$$R_\infty = R'_{\infty\,s}/R'_{\infty\,st} , \quad (2)$$

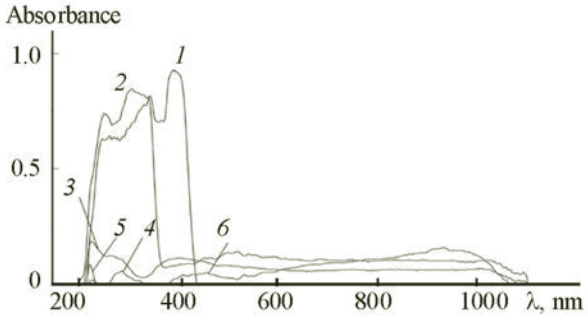


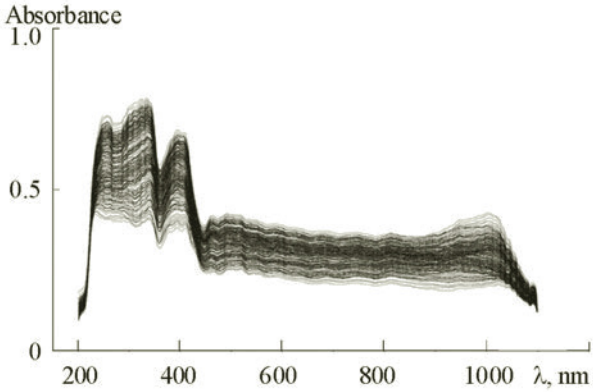


Fig. 1. UV-Vis-swNIR diffuse reflectance spectra of single active component and excipient; 1) amiloride hydrochloride, 2) hydrochlorothiazide, 3) starch, 4) dextrin, 5) sodium carboxymethyl starch, and 6) magnesium stearate.

Fig. 2. UV-Vis-swNIR diffuse reflectance spectra of all artificial tablet samples.

where $R'_{\infty\,s}$, $R'_{\infty\,st}$, and $R_\infty$ are the absolute diffuse reflectance rate of samples and the reference material and relative diffuse reflectance rates, respectively.

Qualitative analysis of a single component helps in establishing calibration models. As shown in Fig. 1, the absorption band of AMH is from 200 to 430 nm, with a maximum absorption wavelength at 400 nm. The absorption band of HCTZ is 200–380 nm with a maximum absorption wavelength at 310 nm. The absorption of each excipient is much weaker than that of the two active components in the range 200–430 nm. The main absorption wavebands of diffuse reflectance for AMH and HCTZ are consistent with those of their UV-Vis absorbance spectra within 200–400 nm caused by the electron transition of the conjugated double bond of N=N, C=N, and C=O. The difference of absorbance in 200–430 nm for AMH and HCTZ plays an important role in the quantitative analysis of components in their compound tablet.

The UV-vis-swNIR diffuse reflectance spectra of all artificial tablet samples are shown in Fig. 2. As can be seen in Fig. 2, the spectra of samples of different contents are similar, with a strong absorption band from 200 to 430 nm. They display an overlap in the majority of the wavebands. The spectral intensity varies with the content of the components. As mentioned in the Introduction, the conventional methods of calculation are not suitable for analyzing the data, so it is necessary to apply chemometrics to get information from the data in order to establish quantitative models.

Quantitative models were established by using Unscrambler ver9.7 and Matalab R2014a ver8.3 software, after the wavelength selection and pretreatment of the spectra. The performance of the models was evaluated by $R^2$ and the root mean square error (RMSE). RMSE is a measure of the average error in analysis, while $R^2$ represents the quality of the predicted values. The closer $R^2$ is to 1 and the smaller RMSE is, the smaller the differences between the measured values and the values predicted by the models. The calculation of $R^2$ and RMSE are as follows:

$$R^2 = 1 - \sum_{i=1}^{n} (\hat{y}_i - y_i)^2 \Big/ \sum_{i=1}^{n} (y_i - \overline{y}_i)^2 \ , \tag{3}$$

$$RMSE = \sqrt{\sum_{i=1}^{n} (\hat{y}_i - y_i)^2 \Big/ n}, \tag{4}$$

where $y_i$ and $\hat{y}_i$ are the sample concentration of the reference and that predicted by the models, respectively, $n$ is the number of samples used for modeling, and $\overline{y}_i$ is the predicted average value of the $n$ samples.

Removal of the uninformative and/or interfering variables contributes to constructing a reliable and interpretable calibration model with good prediction accuracy.

So far, many methods of wavelength variable selection have been used in multivariate calibration. Among these methods, the reversible jump Markov Chain Monte Carlo (RJMCMC) methods introduced in [25] have proved to be quite promising for variable selection. The random frog is a RJMCMC-like algorithm that was originally proposed to be used in gene selection, which is a general strategy for variable selection. Its advantage is that no mathematical formulation is needed and no prior distributions have to be specified like in formal RJMCMC methods, which makes it easier to implement [26].

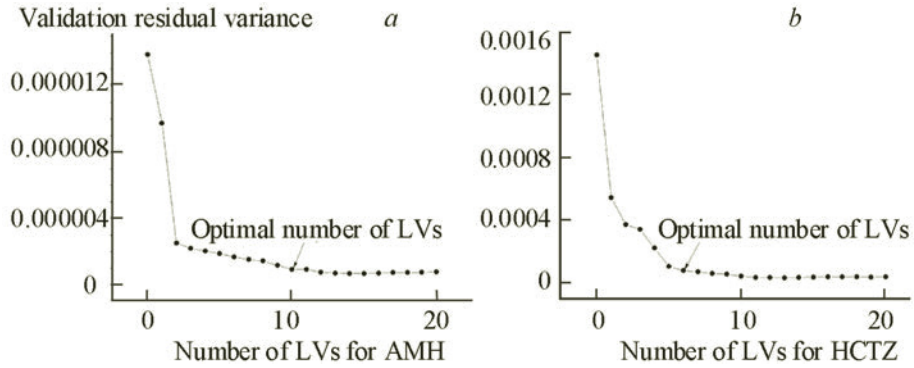


Fig. 3. The relationship between the validation residual variance and LVs for AMH (a) and HCTZ (b).

In this work, the random frog was used for wavelength selection by Matlab R2014a ver8.3. As a result, the 260 and 263 wavelength variables were selected for AMH and HCTZ, respectively.

Ultraviolet-visible spectra contain both sample information and some irrelevant information and noise, such as instrument noise, sample background, and stray light. Therefore, it's significant to choose a spectra pretreatment method to build solid quantitative models.

The original spectra were preprocessed by multiplicative scatter correction (MSC), standard normalized variate (SNV), and Savitzky–Golay convolution smoothing included in Unscrambler ver9.7. In order to avoid overfitting and underfitting, the pretreatment method was chosen by considering $R^2$ and RMSE (RMSEC, RMSECV, and RMSEP) of the calibration set, cross validation, and prediction set. The result showed that the model for AMH and HCTZ established with the spectra preprocessed by Savitzky–Golay convolution smoothing and 1st derivative had a satisfactory effect.

One needs to choose the optimal number of LVs when using PLS algorithm to establish a calibration model. Unsuitable numbers of LVs will lead to the "underfitting" or "overfitting" phenomenon, resulting in an unsatisfactory prediction. LVs were selected by the method of cross validation included in Unscrambler ver9.7 automatically when establishing a PLS model, in which a certain number of samples from the calibration data set are left out and the model is calibrated on the remaining data. Then the left-out samples are predicted and the prediction residuals are computed and all prediction residuals are combined to compute validation residual variance. Figure 3 shows the relationship between the validation residual variance and LVs, and the optimal number of LVs were 10 and 6 for AMH and HCTZ, respectively, considering both calibration and prediction.

The best PLS model was established with spectra preprocessed by Savitzky–Golay convolution smoothing and the 1st derivative with 260 and 263 wavelength variables for AMH and HCTZ, respectively. Figure 4 shows the results of PLS models and effect of prediction. For AMH and HCTZ, the $R^2$ of calibration set was 0.9503 and 0.9538, and the RMSEC was 0.8 and 8.1 mg, respectively. The $R^2$ of prediction set was 0.8983 and 0.9260, and the RMSEP was 1.0 and 8.7 mg, respectively.

The correlation coefficient and random frog methods were both used to select the wavelength variable for SVR modeling. The result showed that the SVR models established with the wavelength variables selected by the random frog had better performance than those established with the wavelength selected by the correlation coefficient method. As a result, the variables of 260 and 263 nm were selected for AMH and HCTZ, respectively.

The pretreatment of spectra was similar to that of PLS modeling. The result showed that the models established with the spectra preprocessed by center and scale had a satisfactory effect.

The parameter optimization of the SVR model was carried out by adjusting the parameter $g$ and regularizing coefficient $c$ and the insensitive loss function $p$ of the kernel function of the radial basis function (RBF). The $g$ value is associated with the degree of confidence or signal-to-noise ratio (SNR) of the sample data; $C$ represents a balance between the complexity of the model (degree of flatness) and the amount of allowed deviation; $P$ controls the width of the insensitive zone and affects the number of support vectors used to build the SVR model [27].

The method of 5-cross validation was used to optimize the parameters. The ranges of values were $g$ [0, 0.03], $c$ [0, 900], and $p$ [0, 0.01], respectively, and the values corresponding to minimal RMSE were regarded as optimal. According to the results of optimization, $g = 0.01$, $c = 900$, $p = 0.0009$ and $g = 0.021$, $c = = 100$, $p = 0.009$ were selected as the optimal

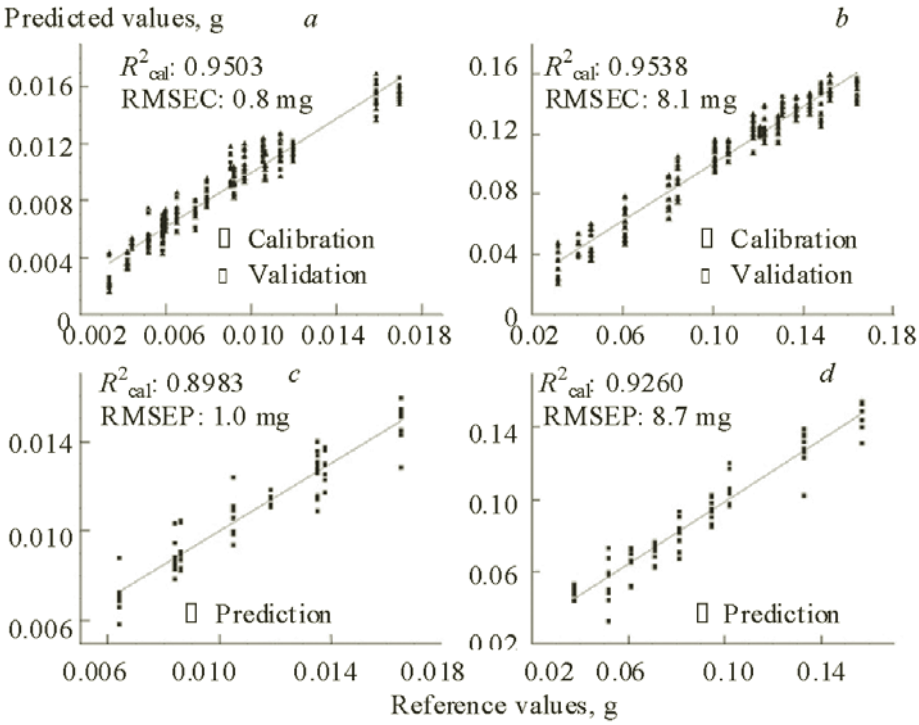


Fig. 4. The results of PLS models of AMH and HCTZ (a, b) and prediction effect of AMH and HCTZ (c, d).

TABLE 1. Effect of Parameter Optimization on the Performance of SVR Models

| Component | Parameter | Calibration | | Prediction | |
|---|---|---|---|---|---|
| | | $R^2$ | RMSEC, mg | $R^2$ | RMSEP, mg |
| AMH | Default | 0.9000 | 1.2 | 0.8769 | 1.3 |
| | Optimized | 0.9668 | 0.7 | 0.9145 | 0.9 |
| HCTZ | Default | 0.8528 | 14.9 | 0.9157 | 11.5 |
| | Optimized | 0.9609 | 7.5 | 0.9446 | 8.9 |

parameters for SVR modeling of AMH and HCTZ, respectively. The performance of SVR models with default and optimal parameters was compared, as shown in Table 1, which indicated that parameter optimization of SVR modeling played a significant role in improving the effect of prediction.

For AMH, $g$ = 0.01, $c$ = 900, and $p$ = 0.0009 were chosen as the optimal parameters and the SVR model was established with 260 wavelength variables preprocessed by center and scale, and the results are shown in Fig. 5a,c. As can be seen, the $R^2$ and RMSEC of calibration set was 0.9668 and 0.7 mg, respectively. And the $R^2$, RMSEP of the prediction set was 0.9145 and 0.9 mg, respectively. For HCTZ, $g$ = 0.021, $c$ = 100, and $p$ = 0.009 were chosen as the optimal parameters, and the SVR model was established with 263 wavelength variables preprocessed by center and scale. The results are shown in Fig. 5b,d. The $R^2$ and RMSEC of the calibration set was 0.9609 and 7.5 mg, respectively. The $R^2$ and RMSEP of the prediction set was 0.9446 and 8.9 mg, respectively.

A comparison of the PLS and SVR models is shown in Table 2. As can been seen, the results of prediction of the two models show that the SVR model had a better effect of prediction. In general, the performance of models for HCTZ established by PLS and SVR was better than that for AMH. Considering that the content level of AMH was lower than that of HCTZ, the results were reasonable. The sources of differences between PLS and SVR models were analyzed as follows:

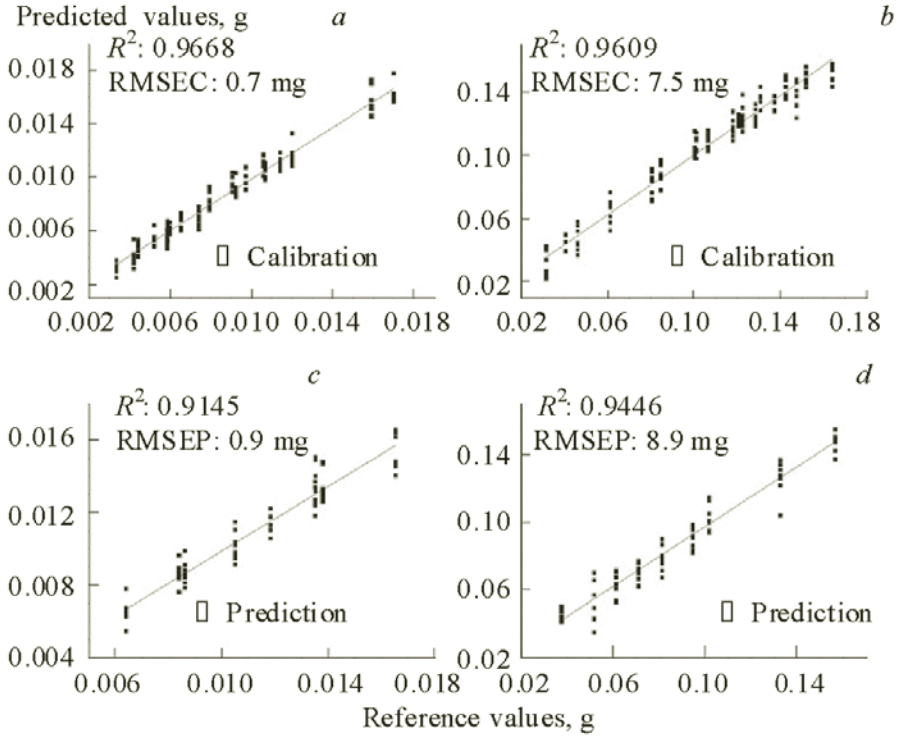


Fig. 5. The SVR models of AMH and HCTZ (a, b) and the effect of prediction of AMH and HCTZ (c, d).

TABLE 2. Comparison of PLS and SVR Models

| Modeling methods | Component | Calibration | | Prediction | |
|---|---|---|---|---|---|
| | | $R^2$ | RMSEC, mg | $R^2$ | RMSEP, mg |
| PLS | AMH | 0.9503 | 0.8 | 0.8983 | 1.0 |
| | HCTZ | 0.9538 | 8.1 | 0.9260 | 8.7 |
| SVR | AMH | 0.9668 | 0.7 | 0.9145 | 0.9 |
| | HCTZ | 0.9609 | 7.5 | 0.9446 | 8.9 |

(a) PLS and SVR are linear and nonlinear modeling methods, respectively; (b) different principles, algorithms, and processing during modeling (wavelength selection and pretreatment of spectra) lead to some differences between the two models.

**Conclusions.** In this study, a simple nondestructive method was developed for simultaneous determination of AMH and HCTZ in a compound amiloride hydrochloride tablet by UV-vis-swNIR DRS and chemometrics. The method has many advantages over the official HPLC and other alternative methods, being lowcost, solvent-free, and nondestructive. The results show that SVR models had prediction performance with $R^2$ of 0.9145 and RMSEP of 0.9 mg for AMH, and $R^2$ of 0.9446 and RMSEP of 8.9 mg for HCTZ. Thus, UV-Vis-swNIR DRS and chemometrics can be used as an efficient nondestructive analytical method for simultaneous determination of multiple active components in compound preparations.

## REFERENCES

1. M. Blanco, J. Coello, H. Iturriaga, S. Maspoch, and C. de la Pezuela, *Anal. Chim. Acta*, **333**, 147–156 (1996).
2. H. M. Albishri, D. Abd El-Hady, and R. A. Tayeb, *Acta Chromatogr.*, **27**, 461–476 (2015).

3. F. Wang and W. Wang, *Jinri YaoXue*, **21**, 81–83 (2011).
4. I. A. Naguib, E. A. Abdelaleem, M. E. Draz, and H. E. Zaazaa, *Anal. Chem. Lett.*, **5**, 85–93 (2015).
5. M. Song, T. Hang, H. Zhao, L. Wang, P. Ge, and P. Ma, *Rapid Commun. Mass Spectrom*., **21**, 3427–3434 (2007).
6. A. G. Jangid, R. H. Tale, and V. V. Vaidya, *Biomed. Chromatogr.*, **26**, 95–100 (2012).
7. I. A. Naguib, E. A. Abdelaleem, H. E. Zaazaa, and M. E. Draz, *J. Chromatogr. Sci.*, **53**, 183–188 (2014).
8. M. Kartal and N. Erk, *J. Pharm. Biomed. Anal.*, **19**, 477–485 (1999).
9. C. V. N. Prasad, C. Parihar, K. Sunil, and P. Parimoo, *J. Pharm. Biomed. Anal*., **17**, 877–884 (1998).
10. M. C. Ferraro, P. M. Castellano, and T. S. Kaufman, *J. Pharm. Biomed. Anal*., **30**, 1121–1131 (2002).
11. M. C. Ferraro, P. M. Castellano, and T. S. Kaufman, *J. Pharm. Biomed. Anal*., **34**, 305–314 (2004).
12. E. A. Abdelaleem, I. A. Naguib, H. E. Zaazaa, and M. E. Draz, *Asian J. Biomed. Pharmac. Sci.*, **34**, 27–33 (2014).
13. M. I. Maguregui, R. M. Jimenez, and R. M. Alonso, *J. Chromatogr. Sci.*, **36**, 516–522 (1998).
14. M. E. Martín, O. M. Hernández, A. I. Jiménez, J. J. Arias, and F. Jiménez, *Anal. Chim. Acta*, **381**, 247–256 (1999).
15. T. Tachikawa, S. Tojo, K. Kawai, M. Endo, M. Fujitsuka, T. Ohno, and T. Majima, *J. Phys. Chem. B*, **108**, 19299–19306 (2004).
16. R. A. Viscarra Rossel, R. N. McGlynn, and A. B. McBratney, *Geoderma*, **137**, 70–82 (2006).
17. J. Brown, K. Vishwanath, G. M. Palmer, and N. Ramanujam, *Curr. Opin. Biotechnol*., **20**, 119–131 (2009).
18. R. A. Schwarz, W. Gao, D. Daye, M. D. Williams, R. Richards-Kortum, and A. M. Gillenwater, *Appl. Opt*., **47**, 825–834 (2008).
19. E. Bertone, A. Venturello, R. Leardi, and F. Geobaldo, *Postharvest Biol. Technol*., **69**, 15–23 (2012).
20. K. H. Kim, S. Jheon, and J. K. Kim, *Spectrochim. Acta, A*, **66**, 768–772 (2007).
21. B. Liang, Y. Y. Feng, H. Song, S. Yao, K. L. Xu, and H. Y. Zou, *J. Sichuan Univ., Eng. Sci. Ed.*, **46**, 182–186 (2014).
22. Y. Y. Feng, X. L. Li, K. L. Xu, H. Y. Zou, H. Li, and B. Liang, *J. Pharm. Biomed. Anal*., **104**, 112–121 (2015).
23. R. Bro, *J. Chemometrics*, **10**, 47–61 (1996).
24. X. Wu and Y. Xie, *Chem. Anal. Meterage*, **18**, 17–20 (2009).
25. P. J. Green, *Biometrica*, **82**, No. 4, 711–732 (1995); http://biomet.oxfordjournals.org/content/82/4/711.short.
26. H. Li, Q. Xu, and Y. Liang, *Analyt. Chim. Acta*, **740**, 20–26 (2012).
27. H. Wu, P. Liu, N. Lü, L. Mu, F. Liu, Y. Zhang, and S. Min, *Chin. J. Pestic. Sci*., **13**, 608–612 (2011).